J. COMBIN. MATH. COMBIN. COMPUT. 127a (2025) 777–791

Journal of Combinatorial Mathematics and Combinatorial Computing
www.combinatorialpress.com/jcmcc

An engineering control design approach based on high-dimensional data analysis in closed-loop systems for industrial networks

Shunping Ji[1,]✉

[1] *School of Mechanical and Electrical Engineering, Sanjiang University, Nanjing Jiangsu, 210012, China*

ABSTRACT

Industrial processes are constantly developing towards large-scale and automation, and the smooth, safe, high-quality, and efficient operation of industrial processes has become a hot spot of concern, and higher requirements have been put forward for the control of production processes. This study analyzes the high-dimensional data in the closed-loop system of industrial network based on the HOPLS-SVM algorithm with higher-order singular value decomposition method. A BP neural network model is constructed with the processed data as the input set to realize the real-time prediction of the main data in the project, and the error of the prediction model is corrected by using linear regression method, and then the project prediction control system is constructed by piggybacking on the model. The results show that the prediction performance of the model in this paper is better than that of the comparison model, and the average absolute error is only 0.0347. At the same time, it is found that the control system in the decomposition project of CHP is able to regulate and optimize the temperature and flow rate of the crude product, which ensures the balance between the product temperature and yield, and the safety of the project operation. The engineering control method designed in this study has strong adaptability and effectiveness, and can provide solutions to engineering control problems in complex industrial processes.

Keywords: HOPLS-SVM, high-order singular value, BP neural network, linear regression method, engineering control

1. Introduction

With the increasing level of networked, automated and intelligent production and life, people have put forward a higher degree of requirements for the performance of actual industrial systems. Under the premise of the booming development of network communication technology and the deepening of the control discipline theory, closed-loop networked control systems (NCSs) have gradually attracted the attention of many domestic and foreign researchers and scholars. Closed-loop networked control systems

✉ Corresponding author.
E-mail address: jishunping1975@163.com (S. Ji).

Received 20 June 2024; Revised 09 September 2024; Accepted 10 October 2024; Published Online 15 April 2025.
DOI: 10.61091/jcmcc127a-045

connect the sensors, controllers, actuators and other nodes in the system through the network, so that data transmission and exchange can be carried out between the nodes, and at the same time can realize the remote control of the system and information resource sharing through the network [1-4]. Compared with the "point-to-point" connection of traditional control technology, the advantages of closed-loop networked control system cover many aspects, such as cost saving, high data transmission efficiency, high reliability, high flexibility, and the realization of information resource sharing, etc. [5-8]. Therefore, closed-loop networked control systems are widely used in various practical engineering projects [9]. However, the actual data in modern industrial closed-loop networked control systems are undergoing great challenges both in terms of scale and dimension, and in the application of high-dimensional data, the amount of computation grows exponentially with the increase in the number of dimensions [10-13]. Unlike monitoring individual data streams, an ideal monitoring solution for high-dimensional data streams requires not only early alerts when certain data streams get out of control, but also the correct identification of these out-of-control data streams [14-17]. Based on this background, the study of engineering control design based on high-dimensional data analysis is of great significance in solving the two major difficulties faced by industrial closed-loop network control systems, namely, the huge amount of data as well as the computational complexity.

In this paper, the engineering control system is designed according to the main characteristics of the industrial network closed-loop system, and the communication of the controller is realized by using TCP/IP protocol and ModBus protocol. The HOPLS-SVM algorithm is constructed by combining the higher-order partial least squares and support vector machine, and the analysis of high-dimensional data in the industrial network system is realized through the computational process of calculating regression function and higher-order singular value decomposition. The analyzed data is used as the input of the BP neural network model, and the nonlinear transformation function Sigmoid function is used to realize the prediction of the main engineering data, and the linear regression method is used to correct the error of the prediction model. Finally, the predictive model is used as the core to build the predictive control module in the engineering control system. This study combines simulation test and case study to explore the application effect of engineering control system.

2. Engineering control realization methods in closed-loop systems for industrial networks

2.1. *Engineering control system structure design*

The structure of the engineering control system in the industrial network closed loop system designed in this paper is shown in Fig. 1. The modern industrial system consists of two parts: hardware device and software system. The hardware device includes the lower computer, reaction kettle, metering tank, mixer, motorized valve, temperature and weight sensors and so on. The reaction kettle is an important reaction vessel in the industrial production process, the metering tank is used to hold liquid chemicals, and the mixer is used to stir the reaction kettle in the production process so that the materials in the reaction kettle are fully reflected. Temperature, weight and other sensors are mainly used to record various information in real time, and the recorded information can be used for the control and prediction of the software system. The software system includes two parts: control system and background management system. The control system is used to control the valve, mixer, so that the material can be accurately titrated, reaction; background management system is used to manage the data, as well as data analysis and prediction. The communication of controller and software uses TCP/IP protocol to communicate, the communication of sensor and controller is divided into two kinds of wired communication and wireless communication, the wired communication uses ModBus protocol [18] to communicate, considering the cost and power consumption, the wireless communication uses the ZigBee protocol based on IEEE802.14 standard to communicate.

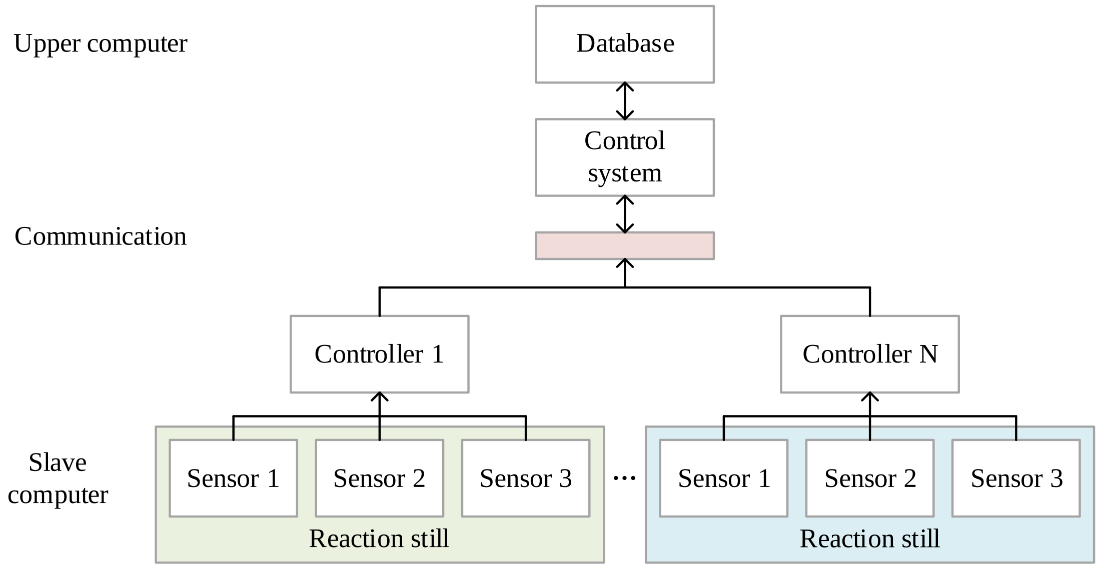

Fig. 1. Industrial control system structure diagram

2.2. Predictive control subsystem establishment

As a sub-system of the background management system in industrial control, the main function of the prediction control system is to be able to automatically predict the changes of temperature, gas concentration and pressure and other factors in the reaction kettle for different industrial production, so as to provide a theoretical basis for the automatic control of engineering. The sequence diagram of the prediction control system is shown in Figure 2. The data source of the prediction control system is the database, and the prediction is made by reading the data in the database. The data in the database is written into the database after reading the values of various types of sensors by controlling the lower computer through the control system. When the control system receives the message to start the industrial production, it sends the signal to the lower computer to start the production and controls the lower computer according to the corresponding production process. In the production process, temperature control is carried out continuously, and messages are sent to the predictive control system in the process of temperature control, so that the temperature of the reactor can be precisely controlled by the predicted temperature. The prediction control system includes four parts: login, parameter setting, model training and prediction control. The feature selection module extracts the factors that have the greatest influence on the changes of material temperature and gas concentration in the kettle in the industrial production line based on the information in the database, and takes them as the feature values. Predictive control module is first trained according to the existing data in the database, and after the training is completed, it can predict the changes of each engineering factor according to the information collected by the sensor to the database in real time. The error correction module can correct the results predicted by the prediction control module to make the prediction results more accurate.

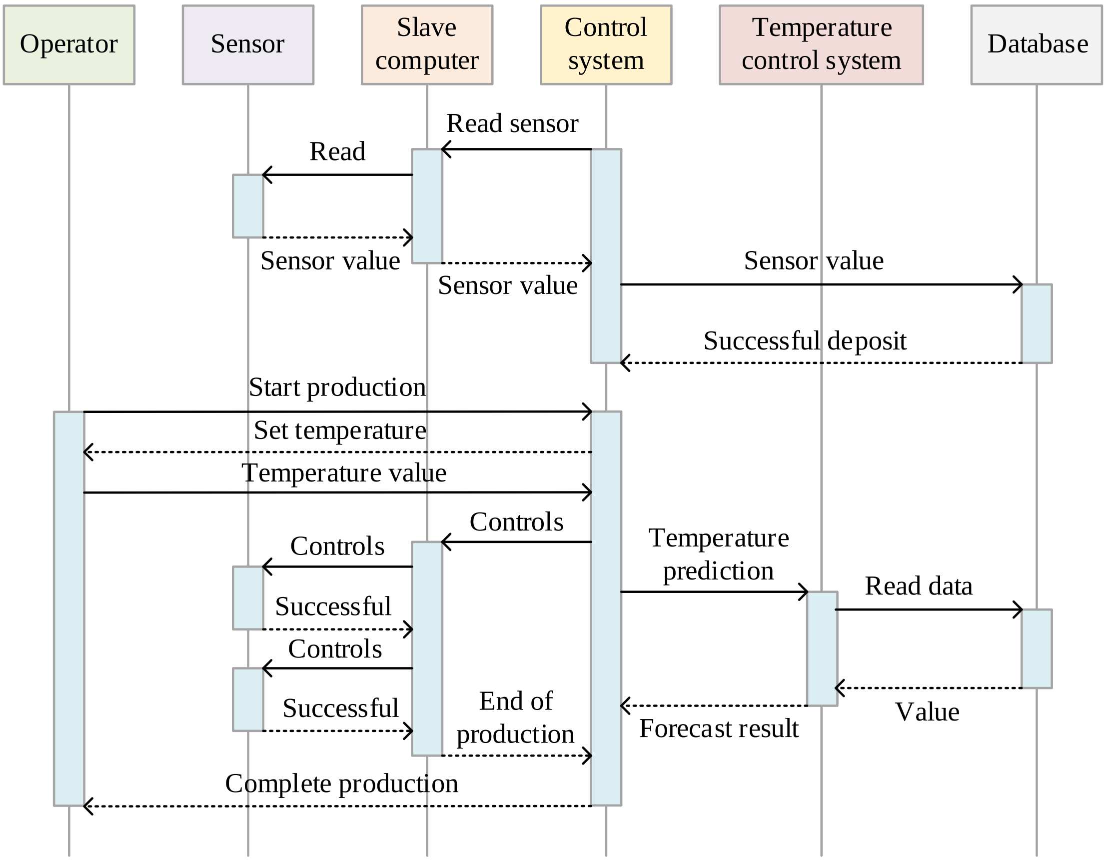

Fig. 2. Prediction system sequence diagram

3. Engineering predictive control methods based on high-dimensional data analysis

3.1. HOPLS-SVM based high dimensional data processing

3.1.1. Construction of the HOPLS-SVM algorithm. Higher Order Partial Least Squares (HOPLS) [19] extends the Partial Least Squares (PLS) algorithm to a higher order and is a novel generalized multilinear regression method. It is characterized by predicting the data by projecting them onto the latent space, thus achieving the purpose of predicting the tensor (or multidirectional array) Y by means of tensor X and regressing the corresponding latent variables. Tensor $\mathrm{X} \in \mathbb{R}^{I_1 \times I_2 \times \cdots \times I_N}$, where N is the order of the tensor X (generally a third order tensor is taken, i.e., $N = 3$), variable I_i denotes the dimensionality of the mode (mode) i, and the response variable $Y \in \mathbb{R}^{I}_{1}$. Higher-order partial least squares differs from other regression models in a number of ways. The orthogonal Tucker model it employs is more robust and adaptable among all types of computational models and can also be applied to a wider range of situations than the CP decomposition. The Tucker decomposition results in a better balance between model adaptability and computational complexity. The introduction of the Higher Order Singular Value Decomposition (HOSVD), a closed form solution, makes the computational process of the new algorithm more computationally efficient than the traditionally used iterations in the past. Support Vector Machines (SVMs) [20] are a class of learning techniques developed to solve the problem of learning from examples. SVMs are used when one needs to approximate a function that cannot be modeled because the underlying mapping is too complex (e.g., meteorological phenomena), or because the function is too costly to evaluate for practical goals, such as finite element simulations. Support vector classification is a special case of supervised learning that deals with models whose output is discrete. Support Vector Machines By implementing the principle of structural risk minimization, support vector machine classification achieves a high degree of accuracy while minimizing the risk of overfitting. SVM algorithms use feature maps to map the input data into a high-dimensional feature space. Based on this, this paper effectively combines the algorithms of HOPLS and SVM to realize the analysis and processing of high-dimensional data in industrial networks.

For large-scale data in the form of tensor in a closed-loop system of industrial network, the training samples and their outputs $\{X_i, y_i\}, i = 1, 2, \ldots, M$ are given by where $X_i \in R^{n_1 \times n_2 \times \cdots \times n_N}$ is the spectral data of a tensor of order N, M is the number of training samples, and $y_i \in R$ is the target value of the output. The regression estimation function is:

$$f(\mathrm{X}) = \mathrm{X} \prod_{k=1}^{N} \times_k \omega_k + b \tag{1}$$

where $\omega_k \in R^{n_k} (k = 1, 2, \ldots, N)$, $b \in R$ are the parameters of the model to be determined and the symbol $\times_k$ is the symbol of the tensor product of the tensor and the vector. For example, the second-order tensor $B \in R^n \times p$ obtained by multiplying the third-order tensor $\mathrm{A} \in R^m \times m \times p$ with the vector $u \in R^m$ is computed with each element of its second-order form $B_{jk} = \mathrm{A} \times_1 u = \sum_{i=1}^{m} A_{vik} u_i, A_{vi}$ as an element of the tensor A. Again with the addition of the insensitive loss function ε, the regression estimation function in Eq. can be turned into the following optimization problem:

$$\begin{cases} \min_{\omega_k, b, \xi, \xi^*} \dfrac{1}{2} \prod_{k=1}^{N} \| \omega_k \|^2 + C \sum_{i=1}^{M} (\xi_i + \xi_i^*) \\ \text{s.t.} \begin{cases} y_i - X_i \prod_{k=1}^{N} \times_k \omega_k - b \le \varepsilon + \xi_i \\ X_i \prod_{k=1}^{n} \times_k \omega_k + b - y_i \le \varepsilon + \xi_i^*, i = 1, 2, \ldots, M \\ \xi_i \ge 0, \xi_i^* \ge 0 \end{cases} \end{cases} \tag{2}$$

The iterative calculation steps of the method are as follows.

1) Let ω_k all element values be 1, $k = 1, 2, \ldots, N-1$.

2) $j = N$.

3) Let $x_i^{(j)} = X_i^T \prod_{k=1} \times_k \omega_k \in R^{n_j}$. Since $\omega_k, k = 1, 2, \ldots, N, k \ne j$ is known, then the optimization problem in Eq. (2) becomes:

$$\begin{cases} \min_{\omega_j, b, \xi, \xi^*} \dfrac{1}{2} \| \omega_j \|^2 + C \sum_{i=1}^{M} (\xi_i + \xi_i^*) \\ s.t. \begin{cases} y_i - X_i^{(j)\tau} \omega_j - b \le \varepsilon + \xi \\ X_i^{(j)T} \omega_j + b - y_i \le \varepsilon + \xi_i^*, i = 1, 2, \ldots, M \\ \xi_i \ge 0, \xi_i^* \ge 0 \end{cases} \end{cases} \tag{3}$$

4) $j = j - 1$, return to step (3) until $j = 1$, and compute $\omega_k, k = 1, 2, \ldots, N$.

5) Return to step (2) and loop the computation of $\omega_k, k = 1, 2, \ldots, N$ until $\omega_k (k = 1, 2, \ldots, N)$ and b obtained from two adjacent loops are close to each other. After the computational process is optimized, the corrected model is obtained from the regression estimation function $f(\mathrm{X})$ based on the computed $\omega_k (k = 1, 2, \ldots, N)$ and b.

3.1.2. Higher-order singular value decomposition. Higher Order Singular Value Decomposition [21] The process decomposition is shown in Fig. 3, Higher Order Singular Value Decomposition (HOSVD) is a natural extension of SVD to third order tensor, $\mathrm{X} = \mathrm{S} \times_1 U^{(l)} \times_2 U^{(2)} \cdots \times_N U^{(N)}$ which can be considered as a special form of constrained Tucker decomposition, where all the factor matrices $B^{(n)} = U^{(n)} \in \mathbb{R}^{I_n \times I_n}$ are orthogonal and the core tensor $\mathrm{G} = \mathrm{S} \in \mathbb{R}^{I_1 \times I_2 \times \ldots \times I_N}$ is fully orthogonal.

The input Nth-order tensor $\mathrm{X} \in \mathbb{R}^{I_1 \times I_2 \times \cdots \times I_N}$ and approximation accuracy ε and the output HOSVD in Tucker format $\hat{\mathrm{X}} = \left[\mathrm{S}; U^{(l)}, \ldots, \underline{U}^{(N)} \right]$ are shown in $\| \mathrm{X} - \hat{\mathrm{X}} \|_F \leq \varepsilon$.

1) $\mathrm{S} \leftarrow \mathrm{X}$
2) for $n = 1$ to N do
3) $\left[U^{(n)}, S, V \right] = truncated_{svd} \left(S_{(n)}, \frac{\varepsilon}{\sqrt{N}} \right)$
4) $\mathrm{S} \leftarrow \mathrm{VS}$
5) end for
6) $\mathrm{S} \leftarrow \mathrm{reshape}(\mathrm{S}, [R_1, \ldots, R_N])$
7) return kernel tensor S, orthogonal factor matrix $U^{(n)} \in \mathbb{R}^{I_n \times R_n}$

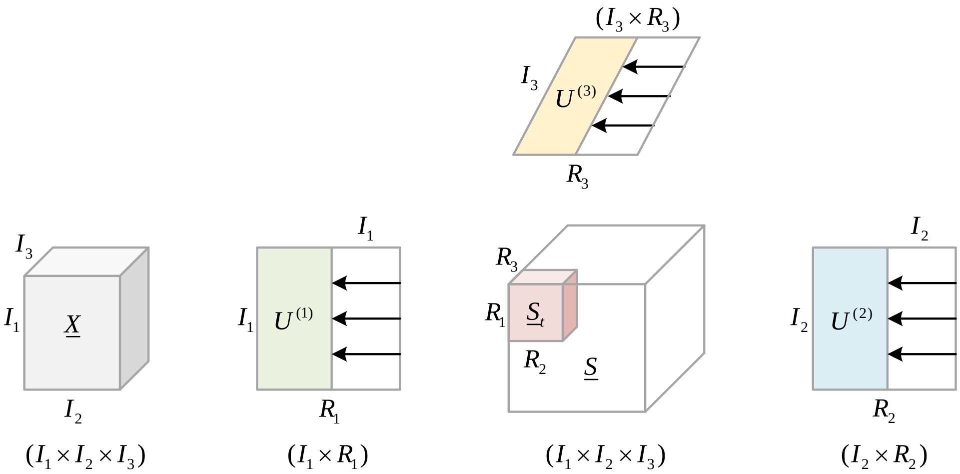

Fig. 3. High order singular Value decomposition (HOSVD) diagram

3.2. *Engineering prediction modeling*

3.2.1. Neuron Transformation Function Selection. In this paper, the transfer function of BP neural network [22] is set as a nonlinear transformation function Sigmoid function [23], and the industrial data after high-dimensional data analysis is used as an input to realize the prediction of the relevant data in the industrial production process based on the BP neural network.

The transfer function of the hidden layer uses a bipolar S-type function, i.e., tansig function. Tansig function corresponds to the mathematical expression:

$$f(x) = \frac{2}{1 + e^{-2\pi}} - 1, (-1, 1) \tag{4}$$

The transfer function at the output layer uses a unipolar S-type function i.e. logsig function. Logsig function corresponds to the mathematical expression:

$$f(x) = \frac{1}{1 + e^{-x}}, (0, 1) \tag{5}$$

Since the S-type functions chosen for the BP neural network, i.e., the tansig function and the logsig function, both require that the input and output vectors are in the range of the interval [-1, 1], the data is normalized before training is performed, and the data is inverse normalized after output.

The normalization formula is shown in Eq:

$$x' = \frac{x - \min}{\max - \min} \tag{6}$$

where x' is the normalized value.

3.2.2. Number of hidden layer nodes. The number of hidden layer nodes will have an impact on the accuracy performance of the entire BP neural network, and there is no accurate theoretical basis for determining the optimal number of hidden layer nodes, can only choose to use empirical formulas to determine the range of the number of nodes in the hidden layer, after the BP neural network performance comparison method to determine.

The empirical formula for determining the number of hidden layer nodes, such as Eq:

$$\begin{cases} m = \sqrt{n+l} + \alpha \\ m = \log_2 n \\ m = \sqrt{nl} \end{cases} \tag{7}$$

Where m is the number of hidden layer nodes, n is the number of input layer nodes, 1 is the number of output layer nodes, and a is a constant between 1 and 10.

3.2.3. Model Error Correction. Due to the characteristics of BP neural network may fall into the local optimal solution, the error correction is carried out for BP neural network. Due to the simple factors affecting the prediction error of the BP neural network and the characteristics of easy to establish mathematical models, the linear regression method is used to correct the prediction error of the BP neural network. After using the prediction error of the BP neural network and establishing a linear regression model, the model can be used to predict the error of the BP neural network. After the initial prediction using the BP neural network, the prediction error is predicted using the error correction model, and then the two results are synthesized to obtain the final prediction results. By performing the simulation, the equation of the linear regression model is established as

$$y = b_0 + b_1 x_1 + b_2 x_1^2 \tag{8}$$

where x_1 represents the time series and y represents the prediction error.

After training for the BP neural network, the trained BP neural network is used to make predictions for another training set, and the difference between the prediction results and the actual results is calculated, which is used as the training set to train the linear regression model. After training, the equation of the linear regression model is obtained as follows:

$$y = -1.0281 - 0.3787x_2 - 0.3883x \tag{9}$$

4. Engineering predictive control system application analysis

4.1. Predictive model feasibility validation

4.1.1. Model performance evaluation indicators. In the reasonable performance evaluation of engineering control prediction models in industrial network closed-loop systems, several appropriate performance evaluation indexes are selected to evaluate the prediction models. The acceptable model training error and the acceptable minimum value of prediction accuracy are not the same because the accuracy predicted by different prediction models varies in different application environments and different data scenarios. Through extensive reading of the literature, it was found that the evaluation criteria are different for each study, and the criteria depend on their own specific application environment related. Three evaluation methods were chosen to evaluate the model, and each error is described as follows.

Mean absolute error performance metrics:

$$MAE = \frac{1}{n}\sum_{i=1}^{n}| y_i^{'} - y_i | \tag{10}$$

Mean square error performance metrics:

$$MSE = \frac{1}{n}\sum_{i=1}^{n}(y_i^{'} - y_i)^2 \tag{11}$$

Mean relative error performance metrics:

$$MRE = \frac{1}{n}\sum_{i=1}^{n}\left|\frac{y_{i'} - y_i}{y_i}\right| \tag{12}$$

In the above three formulas, y_i is the real data value in the industrial production process, $y_i^{'}$ is the data prediction value of the prediction model, and n is the size of the predicted data in the industrial production process.

All three indicators can reflect the overall prediction performance of the model, the average absolute error can better reflect the actual situation of the error between the predicted value and the actual value of the data in the industrial production, and the relative error can more accurately reflect the accuracy and credibility of the data prediction. The root mean square error can reflect the accuracy of data prediction well.

4.1.2. Engineering prediction model performance analysis:

1) Predictive simulation analysis. In this section, the data in a closed-loop system of a refining industrial network is used as the source of simulation data set, and numerical simulation prediction calculations are carried out with the model based on the records of on-site smelting operation and process parameters in the actual industrial production process. The main parameters such as C_{arc}, C_{rs} and convective heat transfer coefficient α between the shell and the atmosphere in the project were adjusted accordingly, so that the calculation results further approximated the measured value of molten steel temperature. Extracted 20 furnace refining end of the measured temperature of the forecast temperature accuracy verification, error analysis results shown in Table 1. The forecast value of the steel temperature at the end of refining agrees well with the measured value, and among the 20 sets of data, 35% of the data (7 sets) have an error of ≤±5°C, and 70% of the data (14 sets) have an error of ≤±10°C. This indicates that the forecast temperature based on the high-dimensional data analysis is more accurate than the measured value. This indicates that the establishment process of the predictive control model based on high-dimensional data analysis is reasonable and the application in engineering control is stable and reliable.

Table 1. Analysis of the prediction of refining industry

Furnace number	Predictive value (℃)	Measured value (℃)	Error (℃)	Furnace number	Predictive value (℃)	Measured value (℃)	Error (℃)
1	1594.53	1601.05	-6.52	11	1584.58	1591.97	-7.39
2	1590.26	1577.99	12.27	12	1561.46	1562.03	-0.57
3	1581.94	1569.08	12.86	13	1594.59	1592.15	2.44
4	1573.97	1574.24	-0.27	14	1596.11	1581.38	14.73
5	1580.31	1583.2	-2.89	15	1598.73	1597.19	1.54
6	1576.94	1583.12	-6.18	16	1584.99	1595.01	-10.02
7	1594.95	1587.52	7.43	17	1559.89	1564.07	-4.18
8	1587.58	1592.65	-5.07	18	1590.18	1582.02	8.16
9	1591.12	1576.93	14.19	19	1574.34	1583.75	-9.41
10	1587.61	1584.73	2.88	20	1589.39	1600.22	-10.83

2) Model comparison analysis. In this paper, we select four methods, LWPLS-1, LWPLS-2, LWPLS-3, and LWPLS-4, which are excellent prediction models in industrial control in related research, as the comparison models, and the results of statistical analysis of the prediction errors of the five methods on the simulation dataset are shown in Table 2. The first method LWPLS-1 has the largest values of all prediction errors (MAE=0.1650, MSE=0.1372, MRE=1.0919), while the prediction errors of the remaining three comparative methods are substantially reduced compared to LWPLS-1. The prediction model based on the high-dimensional data analysis proposed in this paper has the smallest prediction error values for each of the prediction error values (0.0347, 0.0176, and 0.0627), which indicates the best prediction performance among the five modeling methods. Analysis of the reasons shows that since LWPLS-1 does not carry out modeling data updating, while the other three methods have taken sample updating measures, indicating that updating the training samples when the engineering conditions undergo obvious state changes beyond the coverage of the historical samples can effectively maintain the prediction performance of the model and improve the model's ability to adapt to the migration of the process engineering conditions.

Table 2. Model predictability can compare results

Method	MAE	MSE	MRE
LWPLS-1	0.1650	0.1372	1.0919
LWPLS-2	0.0931	0.1270	0.6294
LWPLS-3	0.0550	0.1153	0.5247
LWPLS-4	0.0460	0.0668	0.3638
This article	0.0347	0.0176	0.0627

4.2. *Engineering Optimization Control Case Study*

4.2.1. Engineering control objects. In this paper, the decomposition unit of isopropyl benzene peroxide (CHP) in a closed-loop system of a chemical industry network is used as a study case for engineering control optimization. Isopropyl benzene peroxide (CHP) with a concentration of 80-84 wt% enters from the top of the decomposer, while a water injection pump quantitatively injects cold condensate from a water injection tank into the decomposition feed line to maintain the amount of water required for the decomposition reaction. Sulfuric acid is injected into the recirculation loop as a catalyst for the decomposition reaction. Decomposition crude products are extracted and delivered by crude product pumps, and the delivered products include phenol, acetone, isopropylbenzene, AMS, and water. The decomposition unit has six parameters including reactor tower pressure (28-33 kpa), reactor tower level (27-52%), crude product flow rate (13-25 m^3/h), peroxide isopropylbenzene (CHP) flow rate (11-19 m^3/h), decomposer temperature (condensate control) (50-64°C) and crude product temperature (72-98°C). The decomposition reaction is highly exothermic, and the decomposition generates a large amount of heat that is moved out through the condenser. If the temperature is too high during the reaction, safety accidents are likely to occur, and it will cause a large increase in the amount of tar in the decomposer, clogging the filters and the wall of the attached tubes, reducing the system's continuous operation time, which also increases the number of downtime for maintenance and increases the operating costs. The temperature of the crude product affects the temperature in the decomposer through the cycle. This paper aims to reduce the operating cost and the possibility of accidents, so the temperature of the crude product is taken as the optimization target of the engineering control, so that it can be lowered as much as possible within the permissible range, but at the same time the output of the crude product should be ensured.

4.2.2. Model network training results. The predictive model based on high-dimensional data analysis is first systematically modeled on actual data from the industrial production process of decomposition of isopropylhydroperoxide (CHP). In this paper, 250 sets of field data samples are collected, the first 125 sets are used for system model training, and the second 125 sets are used for model calibration. 20 sets of partial field data samples are shown in Table 3. PIC3004 is the reactor tower pressure control, LIC3005 is the reactor tower liquid level control, FIC3006 is the crude product flow rate, FIC3004 is the CHP flow rate control, TIC3003 is the decomposer temperature monitoring, and TI3005 is crude product temperature.

Table 3. Field data sample

Number	PIC3004 (kpa)	LIC3005 (%)	FIC3006 (m^3/h)	FIC3004 (m^3/h)	TIC3003 (℃)	TI3005 (℃)
1	32.55	38.19	15.83	17.77	58.66	78.96
2	29.88	29.98	21.32	11.26	52.5	84.95
3	28.69	46.76	19.99	16.8	61.34	80.4
4	30.17	51.59	22.98	18.99	60.43	92.16
5	31.56	41.75	15.16	12.53	60.1	80.89
6	30.53	45.72	17.2	16.73	59.51	97.22
7	30.42	34.32	14.83	11.04	55.06	82.36
8	32.81	29.31	17.76	11.8	51.54	77.01
9	31.15	51.08	24.34	17.55	51.88	78.38
10	30.04	38.16	23.43	13.28	61.02	94.92
11	31.73	29.75	23.31	14.92	62.44	90.15
12	30.4	38.29	13.84	11.36	59.72	77.94
13	29.18	44.57	16.21	16.12	61.43	89.23
14	28.75	29.88	15.22	13.39	58.74	86.84
15	30.42	38.5	13.01	15.24	54.29	78.07
16	32.12	33.79	13.59	14.61	58.53	72.7
17	28.22	33.54	18.11	18.36	51.92	89.37
18	31.7	50.9	15.89	15.47	53.42	86.35
19	30.03	50.24	14.71	15.14	53.63	78.76
20	30.09	30.98	22.76	15.86	61.88	96.17

Normalization of the data is done first, which makes the network training faster. In this paper, the data is normalized to between [-1,1] according to their different value ranges. The width of the Gaussian function is 0.1. the error criterion for training termination is defined as the sum of error squares, and training is terminated when it reaches 0.001, with a maximum number of iterations of 100. the calibration error is defined as the sum of squares of the errors of the network outputs and the actual outputs. Its training error curve is shown in Fig. 4, and the output fitting curve is shown in Fig. 5. It can be seen that the process of modeling the CHP decomposition unit by the prediction model based on the analysis of high-dimensional data completes the training of the network with little time-consuming and high accuracy.

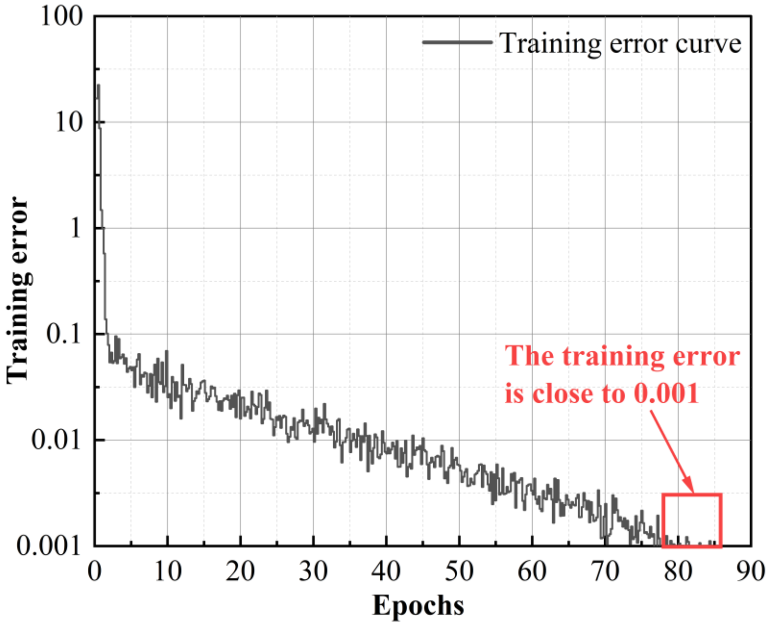

Fig. 4. Training error curve

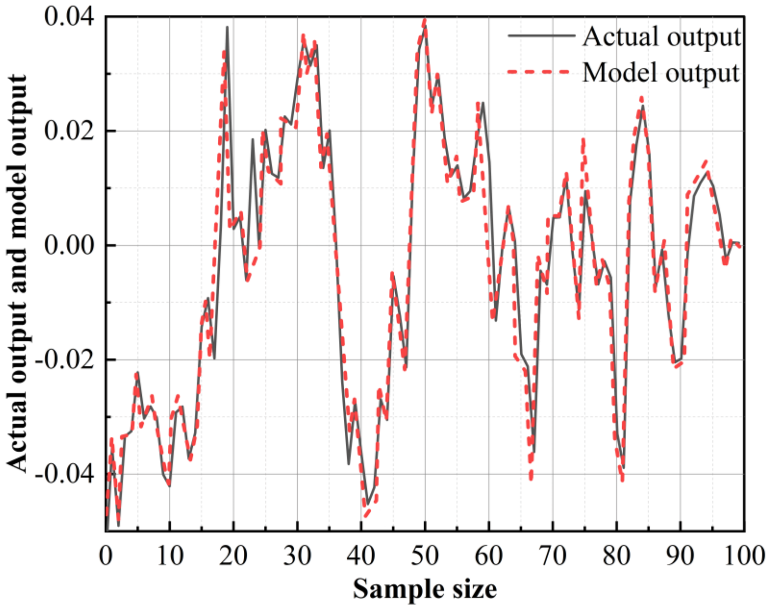

Fig. 5. Output fitting curve

4.2.3. Effectiveness of engineering controls. In this section, an engineering predictive control system based on high-dimensional data analysis is used to regulate and optimize the crude product temperature of an industrial hydroperoxide isopropylbenzene (CHP) decomposition unit. In this paper, the output temperature is considered to be as close to the minimum as possible within the allowable range in order to reduce the possibility of safety incidents. At the same time, the crude product flow rate is kept as high as possible, but not too close to the upper operating limit. The results of the engineering control optimization analysis in the industrial production process are shown in Fig. 6, (a)-(f) represent the changes of PIC3004, LIC3005, FIC3006, FIC3004, TIC3003 and TI3005, respectively. At the industrial production reaction time up to about 19 min, the crude product flow rate in the reactor is too close to the upper limit (24.98 m^3/h), which may bring danger to the operation. The control system proposed in this paper predicts the abnormality through the prediction model and makes timely control and optimization adjustments, which ensures that the flow rate of crude product does not exceed the upper limit (25 m^3/h) on the basis of a high level (24.79-25 m^3/h). At the same time, the temperature of crude product (93.37-93.65℃) is also at a low level. Considering from the perspective of the balance between the product temperature and the output, the engineering control system designed based on the analysis of high-dimensional data in this paper achieves a better application effect.

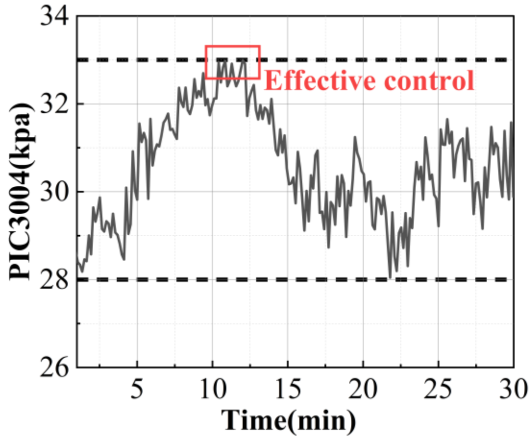

(a) PIC3004

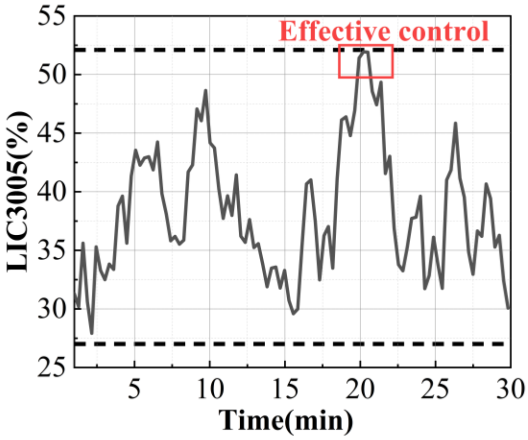

(b) LIC3005

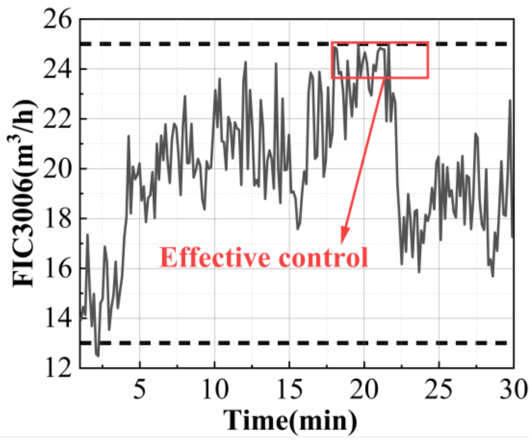

(c) FIC3006

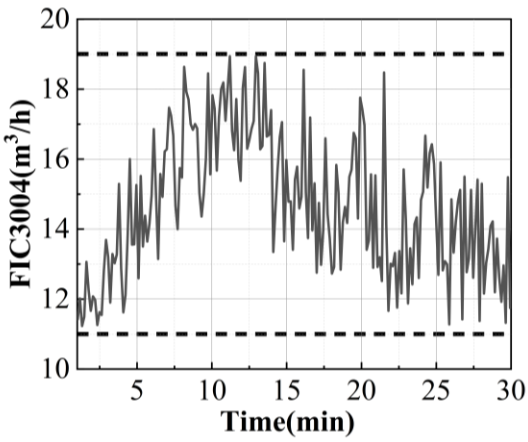

(d) FIC3004

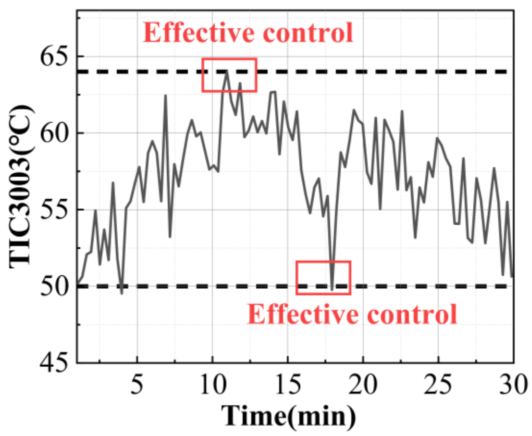

(e) TIC3003

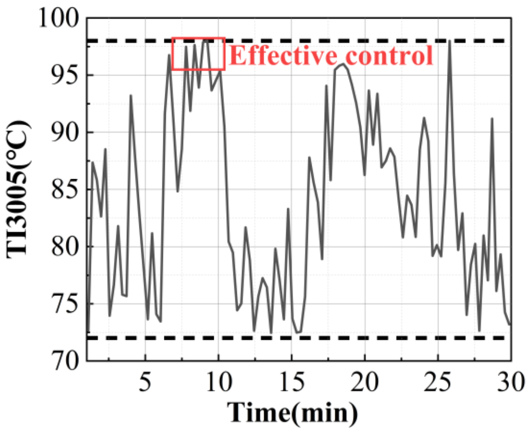

(f) TI3005

Fig. 6. Optimization analysis of engineering control

5. Conclusion

In this paper, the HOPLS-SVM algorithm is used to analyze and process the high-dimensional data in the closed-loop system of the industrial network and input into the BP neural network model to predict the relevant data in the engineering based on the eigenvalues. Then the engineering control optimization system is constructed based on the prediction model. Feasibility validation found that the model's prediction of the temperature in the refining project matches the measured values well, with 35% of the data (7 groups) having an error within ±5°C, and 70% of the data (14 groups) having an error within ±10°C. The prediction error values of each of the predictions are all the smallest (0.0347, 0.0176, 0.0627), and have the best prediction performance among the comparative modeling methods. A chemical industry network closed-loop system, engineering control system is able to regulate and optimize the temperature of the crude product in the industrial hydrogen peroxide isopropylbenzene (CHP) decomposition project, which ensures that the temperature of the crude product (93.37-93.65 ℃) is at a lower level while enabling the flow of the crude product to be at a higher level (24.79-25 m^3/h). The engineering control design method in the closed-loop system of the industrial network designed in this paper can improve the management level of the system, improve the utilization rate of the equipment in the industry, and thus improve the efficiency of the project.

References

[1] Aijaz, A., & Stanoev, A. (2021). Closing the loop: A high-performance connectivity solution for realizing wireless closed-loop control in industrial IoT applications. IEEE Internet of Things Journal, 8(15), 11860-11876.

[2] Huo, M., Luo, H., Wang, H., Jiang, Y., Yin, S., & Kaynak, O. (2022). A distributed closed-loop monitoring approach for interconnected industrial systems. IEEE Transactions on Industrial Electronics, 70(7), 7363-7372.

[3] Gehrke, I., Schauss, M., Küsters, D., & Gries, T. (2020). Experiencing the potential of closed-loop PLM systems enabled by industrial internet of things. Procedia Manufacturing, 45, 177-182.

[4] Özceylan, E., Demirel, N., Çetinkaya, C., & Demirel, E. (2017). A closed-loop supply chain network design for automotive industry in Turkey. Computers & industrial engineering, 113, 727-745.

[5] Bockelmann, C., Dekorsy, A., Gnad, A., Rauchhaupt, L., Neumann, A., Block, D., ... & Ehlich, M. (2017). Hiflecs: Innovative technologies for low-latency wireless closed-loop industrial automation systems. 22. VDE-ITG-Fachtagung Mobilkommunikation.

[6] Santos, A., Lopes, D., César, J., Luciano, L., Neto, A., Guedes, L. A., & Silva, I. (2015, March). Assessment of WirelessHART networks in closed-loop control system. In 2015 IEEE International Conference on Industrial Technology (ICIT) (pp. 2172-2177). IEEE.

[7] Benisha, R. B., & Raja Ratna, S. (2020). Detection of interruption attack in the wireless networked closed loop industrial control systems. Telecommunication Systems, 73(3), 359-370.

[8] Lo Bello, L., Åkerberg, J., Gidlund, M., & Uhlemann, E. (2017). Guest editorial special section on new perspectives on wireless communications in automation: From industrial monitoring and control to cyber-physical systems. IEEE Transactions on Industrial Informatics, 13(3), 1393-1397.

[9] Seijo, Ó., Fernández, Z., Val, I., & López-Fernández, J. A. (2018, June). SHARP: A novel hybrid architecture for industrial wireless sensor and actuator networks. In 2018 14th IEEE International Workshop on Factory Communication Systems (WFCS) (pp. 1-10). IEEE.

[10] Sadoughi, M. K., Li, M., Hu, C., MacKenzie, C. A., Lee, S., & Eshghi, A. T. (2018). A high-dimensional reliability analysis method for simulation-based design under uncertainty. Journal of Mechanical Design, 140(7), 071401.

[11] Du, X., & Zhu, F. (2018). A new data-driven design methodology for mechanical systems with high dimensional design variables. Advances in Engineering Software, 117, 18-28.

[12] Wei, Y., Chen, Z., Ye, Z. S., & Pan, E. (2024). High-dimensional process monitoring under time-varying

operating conditions via covariate-regulated principal component analysis. Reliability Engineering & System Safety, 252, 110440.

[13] Li, M., Sadoughi, M., Hu, C., Hu, Z., Eshghi, A. T., & Lee, S. (2019). High-dimensional reliability-based design optimization involving highly nonlinear constraints and computationally expensive simulations. Journal of Mechanical Design, 141(5), 051402.

[14] Ahmed, F., Mahmood, T., Riaz, M., & Abbas, N. (2024). Comprehensive review of high-dimensional monitoring methods: trends, insights, and interconnections. Quality Technology & Quantitative Management, 1-25.

[15] Liu, H., Wang, X., & Xu, S. (2017). Generalized radial basis function-based high-dimensional model representation handling existing random data. Journal of Mechanical Design, 139(1), 011404.

[16] Zhao, Z., Li, Y., Liu, C., Liu, X., & Gao, J. (2024). Stable Data-Driven Manufacturing Decision-Making by Introducing Causal Relationships for High-Dimensional Data. IEEE Transactions on Industrial Informatics.

[17] Song, X. F., Zhang, Y., Guo, Y. N., Sun, X. Y., & Wang, Y. L. (2020). Variable-size cooperative coevolutionary particle swarm optimization for feature selection on high-dimensional data. IEEE Transactions on Evolutionary Computation, 24(5), 882-895.

[18] Rodríguez Ricardo J.,Marrone Stefano,Marcos Ibai & Porzio Giuseppe. (2023). MOSTO: A toolkit to facilitate security auditing of ICS devices using Modbus/TCP. Computers & Security.

[19] Yuanqing Li,Dianwei Wang,Wuwei Wang,Jiao Wang & Jie Fang. (2024). Correlation mining of multimodal features based on higher-order partial least squares for emotion recognition in conversations. Engineering Applications of Artificial Intelligence(PA),109350-109350.

[20] Xiaochuan Gao,Weiting Bai,Qianlong Dang,Shuai Yang & Guanghui Zhang. (2025). Learnable self-supervised support vector machine based individual selection strategy for multimodal multi-objective optimization. Information Sciences121553-121553.

[21] Qi Zhang,Hong Jiang & Huiming Zheng. (2024). Four-Dimensional Parameter Estimation for Mixed Far-Field and Near-Field Target Localization Using Bistatic MIMO Arrays and Higher-Order Singular Value Decomposition. Remote Sensing(18),3366-3366.

[22] Jiayu Li,Shiwei Jing,Jingfei Cai,Hailong Xu,Pingwei Sun,Yingying Cao... & Guanghao Li. (2025). A method for optimizing different geometric shields of D-T neutron generators by combining BP neural network and Analytic Hierarchy Process. Computer Physics Communications109397-109397.

[23] Qays Adnan Ali,Mohamed Mohamed Elsakka,Nikolay V. Korovkin & Ahmed Refaat. (2024). A novel EPSO algorithm based on shifted sigmoid function parameters for maximizing the energy yield from photovoltaic arrays: An experimental investigation. Results in Engineering102967-102967.